Journal of Visualization, Vol. 3, No. 1 (2000) 37-50

Interferometric Visualization of Jet Flames

Stella, A.*[1], Guj, G.*[2] and Mataloni, A.*[2]

*1 Dip. Meccanica e Aeronautica, Università Di Roma "La Sapienza," Via Eudossiana 18, 00184 Rome, Italy.
*2 Dip. Ingegneria Meccanica e Industriale, Università Di Roma Tre, Via Della Vasca Navale 79, 00146 Rome, Italy.

Received 21 July 1999.
Revised 10 September 1999.

***Abstract*:** This paper presents visualizations of reacting, round jets of the premixed and nonpremixed type realized by using interferometry and, complementarily, direct photography. The available interferometer, proposed by Carlomagno (1986), employs low-cost components and is flexible and robust to geometrical misalignments, allowing the drawbacks limiting the application of traditional interferometric systems to be overcome. Several flames are produced by varying the non-dimensional, governing parameters (Reynolds number, equivalence ratio, Grashof number). The results discussion is organized considering laminar, transitional and turbulent flows. In the steady, laminar case, in view of the radial symmetry of the fringes pattern, the temperature field is reconstructed by the interferograms. The structure of the transitional and turbulent combusting jets, primarily determined by shear layer destabilization mechanisms and large-scale vortices formation due to buoyancy, is analyzed and differences with isothermal flows are pointed out. In turbulent regime, studied only for premixed combustion case, qualitative insights into the structure of the reaction zone as a function of the equivalence ratio and turbulence properties in the incoming fresh mixture are also deduced.

***Keywords*:** interferometry, jet flames, combustion, destabilization, coherent structures.

Nomenclature:

D	burner diameter
F	concentration of fuel
g	modulus of gravity acceleration
Gr	Grashof number
K	Gladstone Dale coefficient
l	aspect ratio of the burner
L	length of the burner pipe
n	index of refraction
O	concentration of oxygen
p	pressure
r	radial co-ordinate of cylindrical frame of reference
Re	Reynolds number
Ri	Richardson number
S	burning velocity
T	temperature
u	local flow velocity component normal to the flame front
V	velocity
x,y,z	Cartesian co-ordinate system

Greek symbols

Δ	variation
ε	angle of divergence of the Wollaston prism
ϕ	equivalence ratio
φ	phase of the electromagnetic wave associated with laser ray
λ	wavelength of the laser source
μ	viscosity
ν	kinematic viscosity
ρ	density
ζ	optical path
ω	vorticity

Subscripts

ad	adiabatic
b	burnt gas state
bar	baroclinic
J	jet
L	laminar
st	stoichiometric
TIP	flame tip
u	unburnt gas state
∞	ambient or reference condition

1. Introduction

The visualization of jet flames has been widely based on the employment of optical methods (shadowgraph, schlieren and interferometry), which are sensitive to spatial inhomogeneities of the refractive index field, as a consequence of density and composition variations. A review of previous applications can be found in Merzkirch (1987), Mungal (1999). The interest towards the application of optical methods is related to the capability of visualizing the topology and the structure of thermal-flow fields (i) in a non-intrusive manner, (ii) without adding tracers to the fluid and (iii) without requiring the availability of a complex and/or expensive experimental set-up, the latter feature being traditionally valid at least for the shadowgraph and schlieren techniques. The first two qualities are particularly attractive for the investigation of combusting flows, involving chemical reactions and intense heat release. The application of interferometry has been rather limited in the past, the main reason being the practical shortcomings deriving from the high sensitivity to geometrical misalignments, which reduces experimental flexibility and forces to employ expensive components (e.g. Mach-Zehnder interferometer, MZI).

A general drawback of the optical methods is that the information is integrated along the optical path. This property limits the capability of earning insights into the local structure of jet flames in turbulent flow regions and where the thermo-dynamic and, consequently, the optical properties of the flowing fluid feature a fractal topology. The interferometry technique gives the possibility to recover local properties from the projection onto a plane, but this procedure is restricted to the case of axisymmetric refractive index fields. Round jet flames exhibit a perfect radial symmetry only in steady laminar cases, which retain a limited interest for technological applications, but having relevant implications for modeling of turbulent combustion.

In this research, we apply the interferometric technique for studying round, reacting jets of the premixed and nonpremixed type. Visualizations are performed in several flow regimes, namely laminar, transitional and turbulent, depending on the characteristic non-dimensional parameters (defined in the following section). In the steady laminar case, the temperature field is also quantitatively reconstructed by the fringes pattern. The available interferometer, proposed by Carlomagno (1986) and used by Guj et al. (1992) and Stella et al. (1999), presents some experimental advantages with respect to classical configurations. First, it allows one to perform reference beam interferometry (RBI) and shearing interferometry (SI) experiments with the same optical configuration by only changing the interferometric unit (a Wollaston prism). Moreover, the interferometer is very robust with respect to geometrical misalignments and gives the possibility to flexibly adjust the configuration to the test flow. A further advantage is the low cost of the mechanical components, since high precision mechanisms for the translational and rotational displacement of the mirrors are not required.

The development of interferometry techniques is a part of a larger research program aimed at the application of non-intrusive, laser based techniques for combustion analysis. In this framework, in addition to the aim of improving physical understanding of the fluid-mechanics involved in reacting jets, interferometry visualizations have been fruitfully used for gaining preliminary assessments on topology and structure of flames for the execution of velocimetry and thermometry measurement campaigns (Stella et al.,1998). In our experience, the joint application of interferometry and Particle Image Velocimetry (PIV) proves to be particularly profitable, mostly due to the complementary character of the results. In fact, while PIV allows the characterization of the inner reaction zone through information concerning both the velocity field and its topology interferometry is effective in providing a global overview of the structure of jet flames, especially in the hot expanding gases region.

2. Visualization Techniques and Set-up

2.1 Interferometry

The interferometer set-up is shown in Fig. 1. It is composed of a rigid optical bench, a 5 mW He-Ne laser source (λ=632.8 nm), a beam expander, a spatial filter, two spherical mirrors with a 0.3 m diameter and a 3 m focal distance, an interferometric unit, an anti-shadowgraph lens, a recording film. The SI is achieved installing a Wollaston prism of quartz with a small angle of divergence (ε=3'). In this arrangement, interference occurs between two conjugate rays both crossing the perturbed refractive index field and separated by a distance (shear) of 2 mm. The RBI is realized using a Wollaston prism of calcite with a large angle of divergence (ε=2.48°) as the splitting unit. In the RBI arrangement, the test section is located on one side of the parallel light beam with respect to the optical axis (as in Fig. 1). One ray passing through the test field (signal ray) and one passing outside it (reference ray) interfere with one another.

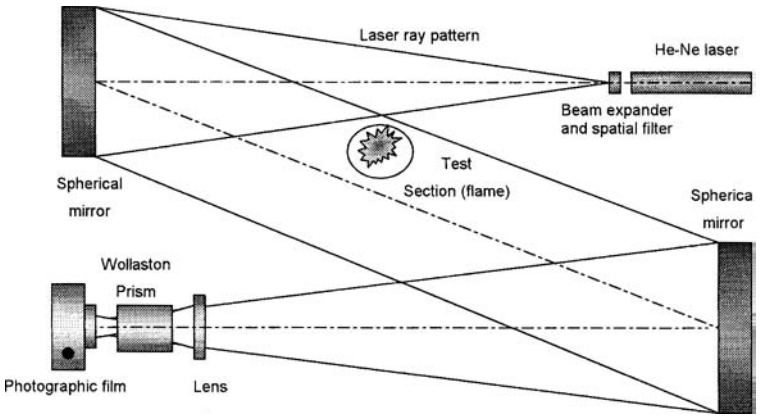

Fig. 1. Experimental setup.

The result of interferometric visualizations consists of a fringes pattern forming in the recording plane. According to the Fermat principle, when a light ray propagates within an inhomogeneous distribution of the refractive index in a fluid medium, it undergoes a phase alteration with respect to that of an undisturbed one. A bright interference fringe forms in the recording plane where the relative phase shift ($\Delta\varphi/2\pi$), corresponding to a relative optical path difference $\Delta\zeta/\lambda$, of the conjugate rays assumes integer values, while a dark fringe appears where $\Delta\varphi/2\pi = \pm 1/2, \pm 3/2...$ A photographic film is employed here to record the fringes pattern. SI measurements are performed adopting the infinite fringe width alignment, that is no fringe is present in the recording plane with a uniform density field, while RBI fringes form over a background system, which has to be taken into account in the evaluation procedure for quantitative reconstruction of the refractive index distribution.

2.2 Direct Photography

The photographic technique has been applied to visualize the luminous structure of flames, used to obtain physical and topological information. A 200 ASA photographic film is used to record the color image of the flame. In the case of nonpremixed flames, a short exposure (1/30 sec) has been selected. In fact, due to soot radiation (as

described in detail in Section 2) the flame acts as an intense light source. On the other hand, a long exposure is needed (1/2 or 1 sec) for visualizing premixed flames, since the intensity of the emitted light is low. This long recording time corresponds to a long integration time with respect to the characteristic time-scales of reacting flows and consequently it affects physical interpretation, as it will be discussed in detail in Section 4.

2.3 Burner

Round, jet flames are produced with a modified burner of the Bunsen type (Fig. 2). The terminal pipe has a constant diameter. Three (1,2,3) pipes with the following diameter (D) and length (L) have been used: D_1=10 mm, D_2=19 mm, D_3=23 mm and L_1=110 mm, L_2=80 mm, L_3=73 mm. The angle of the diverging section located between Bunsen base and pipe reduces with D. In the case of premixed flames, mixing between air and fuel occurs in a cross-flow configuration. The flow rates of air and propane, used as fuel, are fixed through pressure regulators and metered by means of Venturi tubes.

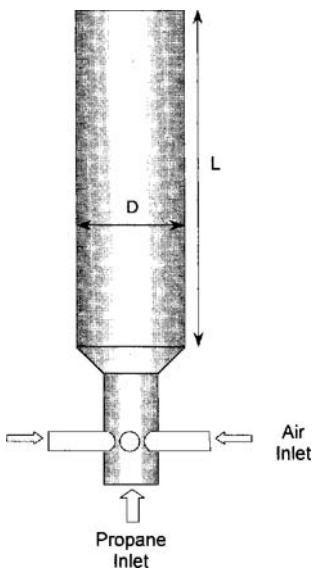

Fig. 2. Schematic of the burner.

3. Physical Model and Governing Parameters

As reviewed by Coats (1997), previous investigations have evidenced that the structure of non-premixed and premixed reacting round jets in the transitional and turbulent regimes is mainly determined by the formation and evolution of coherent, vortical structures. The spectra of time and length scales characterizing the vortical motion in reacting jets differ from the non-reacting case. In vertical jet flames, the destabilization associated with the buoyancy forces is effective in the shear layer between hot gases and the ambient air, where high velocity gradients, due to the acceleration of reaction products as an effect of volumetric expansion, take place. The influence of the buoyancy driven vortices on the inner reaction process and therefore on the global reaction rate differs between premixed and nonpremixed flames, as a consequence of the distinct mechanisms governing the combustion process. In nonpremixed flames, the outer vortices strongly affect the overall reaction rate owing to their stirring action, which promotes mixing of fuel and oxidant on a molecular level, that is the condition for the reaction to occur (Broadwell and Mungal, 1991). Experimental evidences for the occurrence of a destabilization mechanism in the inner side of the reaction surface, presenting an analogy with the one of the Kelvin-Helmotz type, have been deduced by flow visualizations (Yule and Chigier, 1980; Eickhoff and Winandy, 1985; Chen and Roquemore, 1988; Clemens and Paul, 1995). On the other hand, the combustion process in premixed flames is mainly determined by the mechanisms of reaction propagation in the fresh mixture and associated heat release and their interaction with the underlying turbulent flow. The role of large scale, outer vortices in premixed jet flames does not appear to be relevant in most cases for combustion.

In the following we define the independent, non-dimensional parameters which control the physical

phenomena described above and which have been varied during the experiments presented herein.

The dilution of the fuel-oxidant mixture issuing from the burner is expressed introducing the equivalence ratio (ϕ), defined as the ratio between the fuel concentration in the mixture and the stoichiometric value:

$$\phi = \frac{F/O}{(F/O)_{st}}$$

with F and O the concentrations of fuel and oxidant respectively. For a nonpremixed flame, ϕ is equal to ∞, since fuel only flows out from the burner. In the premixed case ϕ is varied between 2.3 and 1.1.

The Reynolds number (Re) takes into account the effect of the jet velocity V_J, of the diameter of the nozzle D and of the kinematic viscosity of the mixture ν:

$$Re = \frac{V_J D}{\nu}$$

The values of ν of air at 15°C (ν=1.460·10^{-5} m^2/s) for premixed flames and that of propane at 15°C (ν=4.14·10^{-6} m^2/s) for diffusive flames are assumed. In the present visualizations, Re ranges between 350 and 2450.

The parameter defining the contribute of the buoyancy forces, which cause the development and drive the large, low frequency, outer vortices is the Grashof number Gr, defined as:

$$Gr = \frac{(T_J - T_\infty) g D^3}{T_\infty \nu^2}$$

with T_J a nominal hot gases temperature, set equal to the adiabatic flame temperature for propane T_{ad}=2170K, T_∞ the ambient temperature equal to 288K, g the modulus of gravity acceleration. In the present tests, Gr is varied from 3.45·10^5 to 2.38·10^7. The ratio between Gr and Re^2 defines the Richardson number (Ri), which gives the relative weight of the buoyancy force with respect to the inertial one. In the present experiments, Ri is varied from 0.04 to 195.

As the geometric, non-dimensional parameter, which affects the velocity profile and turbulence level of the exiting flow, we define the aspect ratio of the pipe:

$$l = \frac{L}{D}$$

For varying the Gr (or Ri) at the same Re different values of l are used: l_1=11, l_2=4.5, l_3=3.2.

4. Results

4.1 Visualizations of Steady, Laminar Flames and Temperature Fields

4.1.1 Reconstruction of axisymmetric temperature fields from the fringes pattern

Radially symmetric refractive index distributions $n(x,r)$ are reconstructed from the projection onto a recording plane, parallel to the x-y plane (the adopted co-ordinate systems are shown in Fig. 3), and the relative interferometric fringes system. Details on measurement procedure, sensitivity and accuracy of the method for temperature determination are provided by Stella et al. (1999). First, the radial variation of $\Delta\phi/2\pi$ for a fixed x coordinate is determined by the fringes distribution and then the inverse Abel transformation (Vest, 1974) is applied to resume the information integrated along the optical path (z direction). Once $n(x,r)$ is known, the density distribution $\rho(x,r)$ can be calculated throughout the Gladstone-Dale relation (Merzkirch, 1987):

$$n(x,r) - 1 = K(x,r)\rho(x,r) \qquad (1)$$

where K is the Gladstone-Dale coefficient. It has to be remarked that while for premixed combustion K can be assumed uniform in the entire field (Merzkirch, 1987; Stella et al., 1999), the space-dependence due to compositions variations can not be neglected in the nonpremixed case. The method of the conserved properties proposed by Weinberg (1963) and used by Pandya and Weinberg (1964) is therefore employed in the present measurements in order to account for composition effects on the $\rho(x,r)$ distribution. Finally, the temperature field $T(x,r)$ for a thermotropic flow is determined recalling the state equation for the gaseous mixture.

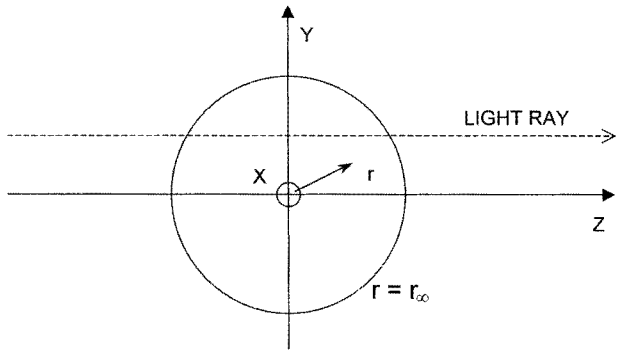

Fig. 3. Co-ordinate systems.

4.1.2 Premixed flame

The RBI and SI visualizations of a premixed flame and the corresponding direct photograph at the same scale, produced with the following values of the governing parameters: Re = 480, Ri=3.5, ϕ=1.1 and l = 4.5, are shown in Fig. 4. In the photographic image, the effect of the long exposure consists of thickening the visible surface of reaction, which slightly vibrates due to low intensity fluctuations.

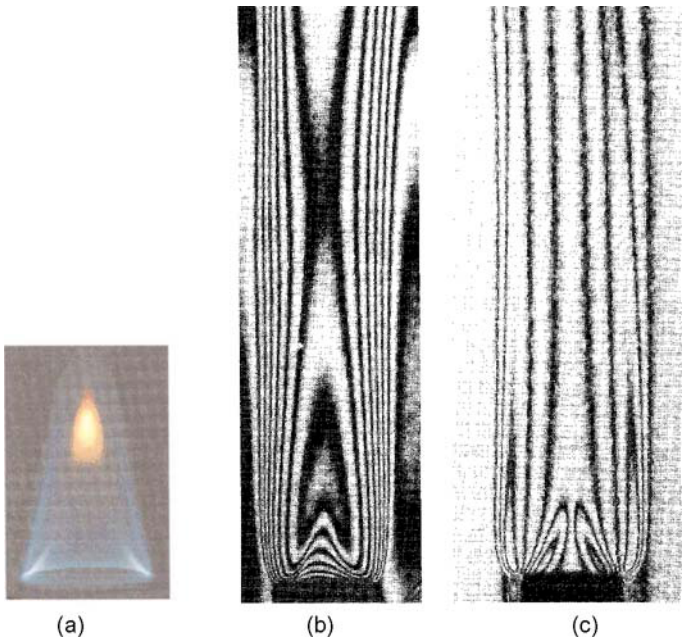

Fig. 4. Visualization of a premixed laminar flame (ϕ =1.1, Re = 480, Ri =3.5, l = 4.5): (a) Direct photograph; (b) RBI visualization; (c) SI visualization.

The laminar flame presents a double structure: an inner cone, attached at the top of the burner, where a pure premixed combustion process takes place, and an outer reaction zone, where the excess fuel burns supported by the surrounding ambient air. A steady situation establishes in the reacting jet since the burning speed S_L, that is the velocity at which the reaction propagates in the fresh mixture, is balanced by the normal component of the local flow velocity to the flame front. Interferometric visualizations reveal symmetry of the thermal structure of the jet persisting also in the hot expanding gases region. The comparison of the direct photography of the flame and the RBI and SI visualizations points out the correlation between the fringes distribution and the physical structure of the flow, as it appears from light emission. The gray streak on both sides of the burner in the SI visualization gives the idea of the separation between two interfering rays (shear).

The calculated temperature map is shown in Fig. 5. The structure of the flow, including (moving along the

x direction from the burner exit): the isothermal cold core of preformed reactants, the preheating zone, the conical reaction surface and the hot plume in the products region is readily pointed out. The maximum temperature exceeds 2000K and is reached gradually moving downstream, probably due to the slowness of the reaction for CO_2 formation. At the flame base the reduced temperature rise at the reaction surface, observed also in previous works (e.g. Law, 1988) is due to the non-adiabaticity of the system for the conductive heat transfer to the burner walls. At the flame tip the temperature is lower than at the shoulder of the reaction cone and well below T_{ad}. This lower temperature region corresponds to the yellow brush appearing in the direct photography, due to soot production and meaning a local richening of the mixture ($\phi_{TIP} > \phi$). This alteration of the flame response at the tip originates as an effect of the flame stretch, induced by the high curvature of the reacting front, in presence of preferential diffusion (as described by Law, 1988), leading to the reduction of the local reaction rate. This motivates, together with the radiative heat losses, the observed fluid cooling at the tip.

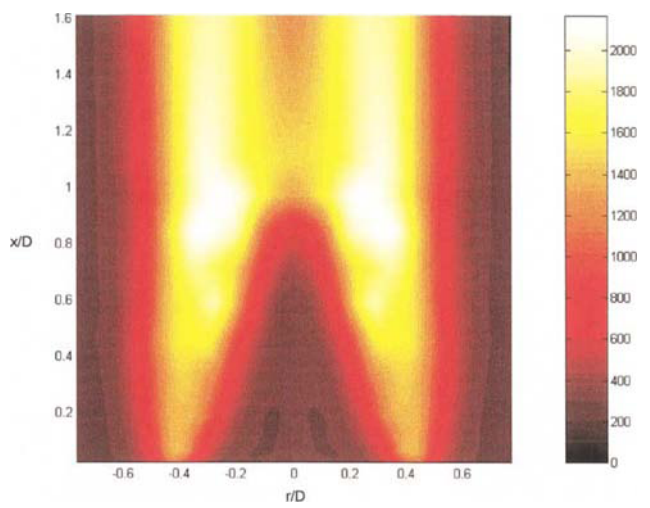

Fig. 5. Temperature map of a premixed laminar flame (ϕ=1.1, Re=730, Ri =3.5, l =4.5).

4.1.3 Nonpremixed flame

The SI and RBI visualizations and the direct photograph of a laminar diffusion flame, at Re=350, Ri=195, l=4.5, is shown in Fig. 6. Chemical reactions and associated heat release take place along a thin surface where oxidant and fuel encounter with one another in a stoichiometric ratio and approximately corresponding to the edge of the yellow brush. The structure of the reaction surface is characterized by two main zones. The former, emitting blue light and poorly visible due to the short exposure, extends from the burner rim to the base of the luminous yellow brush. This zone is very thin because a fast chemistry process takes place. The blue color is due to O_2 emission and is caused by ion recombination. The other upper region appears as a yellow brush owing to the combustion of solid carbon particles and soot emission, behaving as a black body.

The temperature field, deduced by the interferometric visualizations, is shown in Fig. 7. In laminar steady nonpremixed flames, the basic processes sustaining combustion, that are (i) mass transport of reactants to fulfill the mixing condition at the molecular level and (ii) heat transfer needed to preheat the incoming reactants, are driven by molecular diffusion. The reaction surface location coincides with that of the temperature peaks in the map of Fig. 7. The maximum temperatures are reached where soot radiation is more intense (in the interval x/D= [0.79, 1.84]) and are close to T_{ad}. The slightly lower value is consistent with the actual non-adiabaticity of the combustion process, in view of radiative heat loss. In analogy with the premixed case, the conductive heat exchange with the burner walls produces a cooling of the flow with an associated temperature decay in the proximity of the burner.

4.1.4 Interpretation of fringes systems

Some observations on the fringe system configuration and its association with the visualized temperature distribution can be highlighted, having also a certain usefulness for the qualitative interpretation of the interferometric visualizations of round jets in the transitional and turbulent regimes presented in the following. In those cases, indeed, the condition of radial symmetry is no longer applicable and quantitative information can not be obtained. Looking at Fig. 4(c), a concentric path of the SI fringes is observed in the cold fresh mixture zone

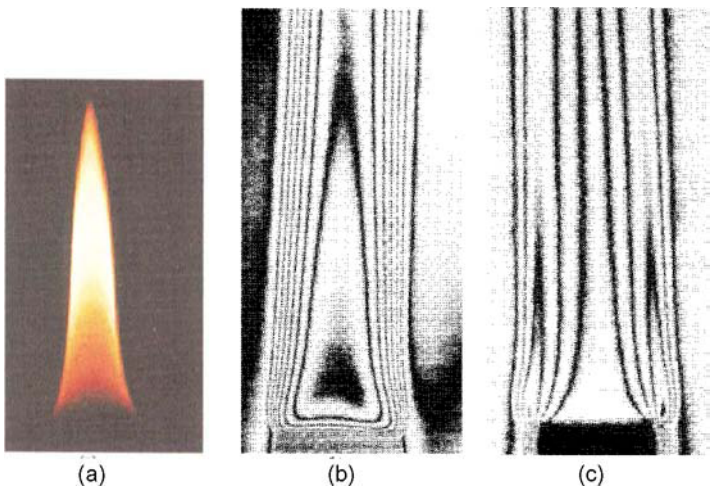

Fig. 6. Visualization of a nonpremixed laminar flame (*Re*=350, *Ri* =195, *I* =4.5): (a) Direct photograph; (b) RBI visualization; (c) SI visualization.

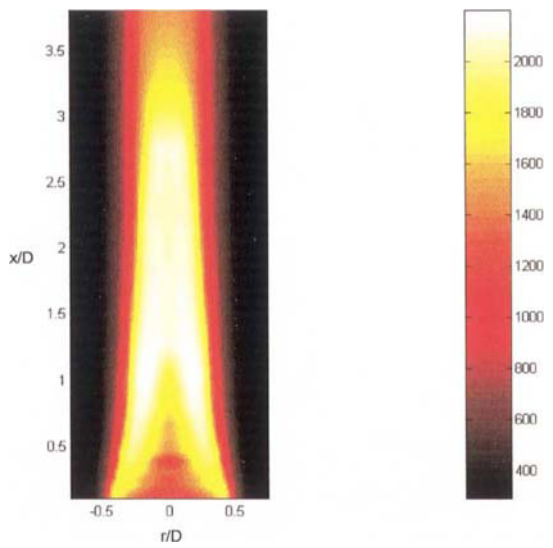

Fig. 7. Temperature map of a nonpremixed laminar flame (*Re*=350, *Ri* =195, *I* =4.5).

even if the temperature field is uniform in that region. Similarly, several fringes, deformed to follow the conical shape of the flame front, appear in the RBI visualization (Fig. 4(b)) in this isothermal zone. The observed fringes patterns, which would instead mean a non-uniform temperature distribution if the visualized flow was planar, are due to the increasing of the light integration length moving towards the jet centerline. As general ideas for better interpreting forthcoming visualizations, one may note that the concentric pattern of the SI fringes and the deformation of the RBI ones at the flame base are significant of the inner side of the reaction surface in the fresh reactants.

Another relevant aspect for the application of interferometry to combusting flows is that both the SI and RBI techniques are more sensitive in regions of low temperatures. In fact, the relative optical path $\Delta\zeta/\lambda$ (and therefore the number of interferometric fringes forming in the recording plane) is dependent on n and $\partial n/\partial r$ for SI and RBI respectively (see Stella et al., 1999 for details) in the case of axisymmetric fields. Thus, recalling the Gladstone-Dale relation and the equation of state for the gas mixture, the refraction index and its first derivative can be related to the temperature as follows:

$$n \propto \rho \propto \frac{1}{T}$$

$$\frac{\partial n}{\partial y} \propto \frac{\partial \rho}{\partial y} \propto -\frac{1}{T^2}\frac{\partial T}{\partial y}$$

for the SI and RBI respectively. It can be seen that in the RBI case the sensitivity reduction with temperature tends to be balanced where high temperature gradients occur. As a result the RBI technique is expected to be rather sensitive in the preheating zones at the shoulders of the flame front. The dependence of sensitivity on temperature represents a shortcoming in the visualization of flows with intense heat sources, especially in hydrocarbons flames where the temperature may vary of a factor up to 5-7 in the field.

4.2 Transitional Flames

4.2.1 Premixed flames

The SI visualization presented in Fig. 8 is produced at Re=480, Ri=21.5, ϕ=1.1 and l=3.2. The fringes pattern at the flame base points out a regular and symmetric structure of the thermal-flow field, analogous to the one obtained for the lower Ri case (Fig. 4(c)). In the hot gases region, the destabilization of the shear layer occurs due to the higher buoyancy forces with respect to the previous case, generating vortical structures whose core dimension is of the order of D, as revealed by the concentric pattern of the SI fringes. A radial symmetry of the fringes pattern is no longer seen in the hot plume. By looking at several visualizations at the same conditions (not shown for brevity), the axial position where flow destabilizes is observed to be approximately constant and the developing vortical structure seems to exhibit a steady nature.

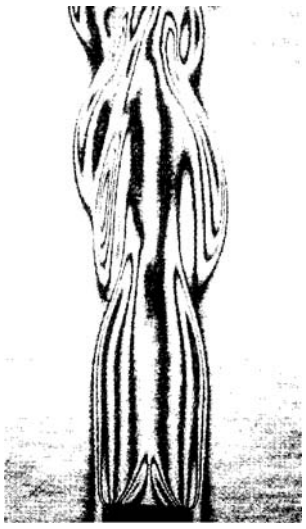

Fig. 8. SI visualization of a premixed flame in the transitional regime (ϕ=1.1, Re=480, Ri =21.5, l =3.2).

4.2.2 Nonpremixed flames

The visualization of a nonpremixed reacting jet in the transitional regime is shown in Fig. 9, for Re=980, Ri=4 and l=11. The development of buoyancy-driven structures produces a large-scale vortical motion, which maintains an almost laminar fashion. This is pointed out by the nearly perfect symmetry of the fringes pattern, which ceases downstream the point where vortices start forming. The onset of the outer shear layer destabilization is disclosed by the wavy path of the jet edges. In spite of the distinct nature of the destabilization process, interesting considerations can be deduced by comparing the structure of the reacting flow with that of an isothermal jet in the regimes where annular vortices form (Re>1500, Becker and Massaro, 1967). Two main aspects can be highlighted. The former one regards the destabilization point, where the roll-up process develops, which is significantly moved downstream in the reacting case. A second aspect is related to the range of spatial scales characterizing the two situations. The wavelength of the vortical structures observed in the jet flame is about 5D, while in the isothermal case the characteristic dimension is of the order of the jet diameter D. This difference is interpreted as an effect of the variation of Re and the influence of Ri in reacting flows, due to the temperature increase. A decreasing Re

results from the increment of the viscous forces, the dynamic viscosity being dependent on the local temperature. Assuming a variation in agreement with the Sutherland law:

$$\frac{\mu_b}{\mu_u} = \frac{T_u + 120}{T_b + 120}\left(\frac{T_b}{T_u}\right)^{1.5} \tag{2}$$

where the subscripts u and b indicate the unburnt and burnt states, and considering T_u=288K and T_b=T_{ad}, μ_b is about 3.7 times μ_u. Under the steady state hypothesis the conservation of mass gives the product ρu, where u is the local flow velocity component normal to the flame front, to be constant across the flame front; hence, a drop in Re occurs. The destabilization driven by the buoyancy forces is also enhanced by the increment of the characteristic length in the post-flame region (about 2D) and the drop of Re, which cause a significant increase of the actual Ri.

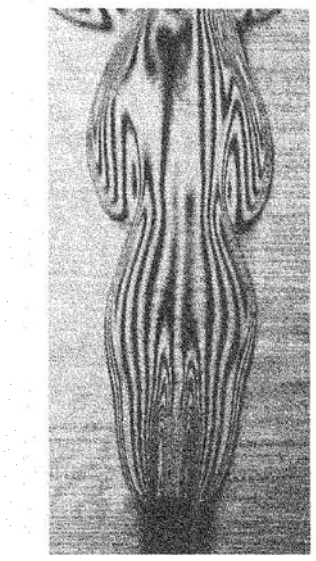

Fig. 9. SI visualization of a nonpremixed flame in the transitional regime (Re=980, Ri =4, l =11).

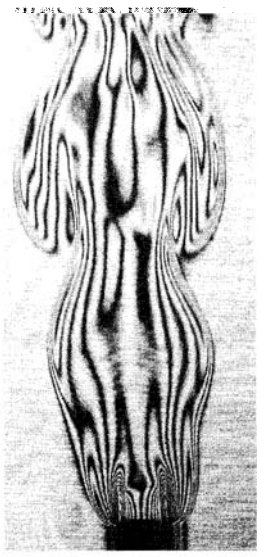

Fig. 10. SI visualization of a nonpremixed flame in the transitional regime (Re=980, Ri =28, l =4.5).

We now propose an evidence on the effect of Ri, which is assessed by only changing the Gr at fixed Re, using a larger diameter nozzle (D_2) and smaller outflow velocity. Figure 10 shows the SI visualization of a nonpremixed flame with a Ri equal to 28. The larger Ri implies stronger buoyancy forces. A relevant difference concerns the destabilization point, that is anticipated to around 5D. No significant variations of the characteristic spatial scales of the vortices, when nondimensionalized with respect to the jet diameter, are instead seen as an effect of Ri. The regular fringes pattern observed in the jet core for the l=11 case (Fig. 9) is no longer observed in the visualization of Fig. 10, suggesting the occurrence of a transitional flow also in the inner regions. This difference could be an effect of (i) the unsteady buoyancy-driven ring like vortices which can destabilize the inner shear layer of the jet and also of (ii) the higher intensity of the incoming flow turbulence, measured by an anemometric technique.

4.3 Turbulent Premixed Flames

Visualizations of premixed reacting jets in the turbulent regime are performed considering a combustion process of the premixed type. The topology of the inner reaction surface and the overall reaction rate modifies significantly for increasing Re with respect to the laminar condition. When framed within the diagram of premixed turbulent combustion regimes, defined basing on the comparison between characteristic scales of chemical process and turbulent motion (see Poinsot et al., 1991; Peters, 1999), the flames visualized in this work fall within the flamelet regime. This means that fresh reactants and products are separated by a thin reacting sheet (flame front), which is wrinkled and eventually corrugated (that is pockets of reactants may appear in the products zone) by the action of turbulent motion.

SI visualizations of premixed, reacting jets are shown in Fig. 11, corresponding to the same parameters Ri=1, Re=1350, l=3.2 and differing for the dilution of the fresh mixture, being ϕ=1.4, ϕ=1.6, ϕ=1.9 in Fig. 11(a),

11(b) and 11(c) respectively. The direct photography of the flame in the case ϕ=1.6 is also shown in Fig. 12. As a result of the long integration time of the incoming light a blue brush at the flame base is seen. The inner fringes system reveals the reaction zone. As discussed above, its detailed topology cannot be reconstructed due to the line-of-sight integration. Nevertheless, some aspects concerning the structure of the reacting surface can be qualitatively inferred. A first relevant feature is its increasing complexity as the actual process approaches a stoichiometric one. This modification of the flame front topology can not be ascribed to the incoming turbulence properties, substantially unaltered in the three cases under consideration. In our understanding, an important role may be played by vorticity production through the baroclinic term of the vorticity transport equation:

$$\left.\frac{D\omega}{Dt}\right|_{bar} = \frac{1}{\rho^2}(\nabla\rho \times \nabla p) \tag{3}$$

This is consistent with the fact that as ϕ is reduced the density gradient is increased, owing to the contemporary reduction of the reaction front thickness and the higher heat release. This speculation is strengthened by the quantitative results obtained by Mueller et al. (1998), who studied the evolution of a vortex crossing a flame front.

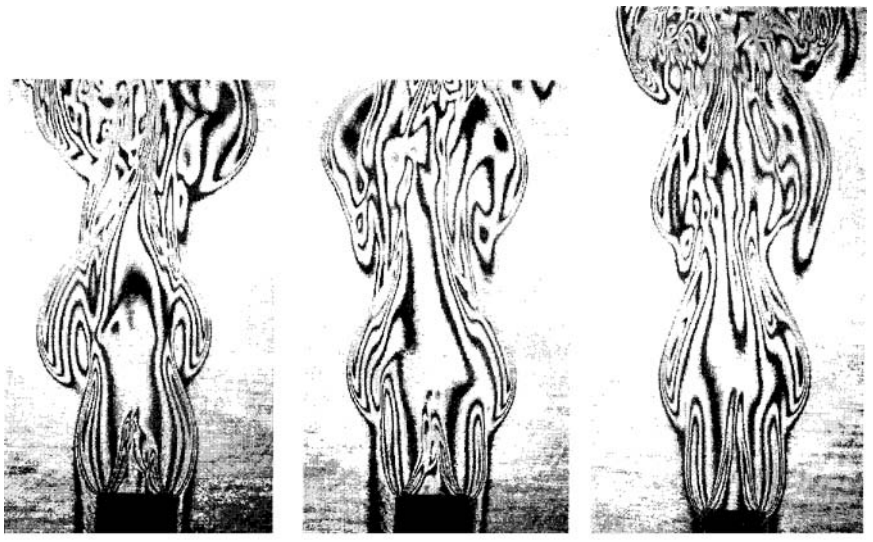

Fig. 11. SI visualization of premixed turbulent flames (*Re*=1350, *Ri* =1, *l* =3.2):
(a) ϕ=1.4; (b) ϕ=1.6; (c) ϕ=1.9.

Fig. 12. Direct photograph of a turbulent flame (ϕ=1.6, *Re*=1350, *Ri* =1, *l* =3.2).

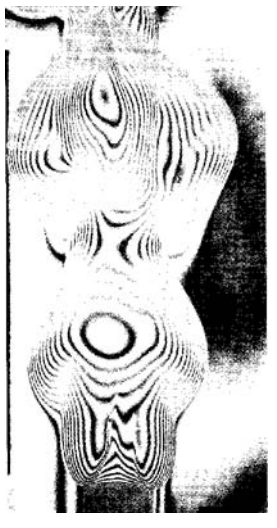

Fig. 13. RBI visualization of a premixed turbulent flame (ϕ=1.6, *Re*=1350, *Ri* =1, *l* =3.2).

A second evident aspect is the shortening of the reaction zone as ϕ approaches ϕ_{st} due to the enhancement of the burning speed and meaning the more intense combustion process. The enlargement of the fringes pattern at the flame base, seen for decreasing values of ϕ, is produced by the larger amount of heat released. In fact, the density drop across the reaction front induces streamlines refraction (see for example Chomiak (1990) for a more detailed explanation), causing the flow to spread outwards in the post-flame region. The streamlines deviation angle increases as the stoichiometric condition is approached in view of the higher density drop.

The shear layer dynamics in the zone where hot gases expand is still characterized by a destabilization process originating large-scale, coherent structures. A reduced influence of ϕ is seen and a steady nature of the vortical structure can be assessed by observing several instantaneous visualizations. This feature can be also noticed comparing the SI visualization of the flame corresponding to ϕ=1.6, with the RBI one proposed as an example of the fringes pattern attainable by using this technique and shown in Fig. 13.

SI visualizations of flames produced through the smaller diameter nozzle (l=11), at Re=2450 and Ri=0.05, with different equivalence ratios (ϕ=2.3 and 1.7 respectively) are shown in Fig. 14. The trace of the inner reaction surface (Fig. 14(a)) provided by the fringes pattern in the core of the jet extends for a long distance in the flame with ϕ=2.3, consistently with the fact that the mixture is rich and l is high enough to give a low turbulence level in the jet flow. In correspondence to the destabilization point of the outer shear layer the tip of the flame becomes unsteady, as evidenced by the oscillating motion of the fringes, causing a gray brush. In the reacting jet under consideration, being an intermediate case between a premixed and a nonpremixed process due to the high fuel concentration, an effect on the interior combustion process by the outer vortices can be noticed. In the ϕ=1.7 case, the SI visualization shows the significant shortening of the burning zone and its unsteady nature (gray brush), readily appearing in the upper part. The enlargement of the outer fringes pattern at the base of the jet is also evident. The comparison with the visualization of Fig. 11, gives the sense of the reduced weight of the buoyancy forces (the Ri is two orders of magnitude lower here). The destabilization point is indeed moved downstream when its height is referred to the nozzle diameter. As soon as the large-scale structure has formed, the transition to unsteady laminar flow originates and the interaction among the large structures can produce a turbulent flow condition, which can be argued by the complex fringes pattern. Local information and fine-scale structures effects are unrecoverable in this turbulent region within the hot plume.

At around the same Re and ϕ values (Re=2320, ϕ=1.5) a partial lift-off condition (visualized in Fig. 15) can establish, since the flame is close to a stability limit and therefore a small perturbation can give rise to separation from the burner rim. Flame ignition takes place at a certain distance from the exit (about $0.8D$ in this case), as indicated by the appearance of an inner fringes pattern at the jet base in the right-hand side. The preheating of the

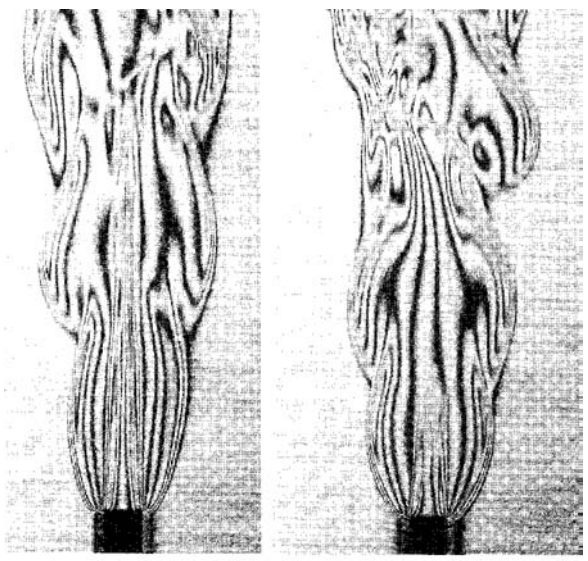

Fig. 14. SI visualizations of premixed turbulent flames (Ri =0.05, l =11):
(a) ϕ=2.3, Re=2450; (b) ϕ=1.7, Re=2450.

Fig. 15. SI visualization of a premixed flame in lift-off condition (ϕ=1.5, *Re*=2315, *Ri* =0.06, *l* =11).

fresh mixture in front of the ignition point is revealed by the upstream prolongation of the outer concentric fringes system towards the center of the jet. The symmetry of the coherent structures forming in the post-flame region is lost and a turbulent plume develops.

5. Final Remarks and Conclusions

The interferometry technique has been applied to visualize reacting, round jets of the premixed and nonpremixed type. Complementarily, direct photography has been also employed. Several flames have been visualized, varying the non-dimensional governing parameters (Reynolds number (*Re*), equivalence ratio (ϕ), Grashof number (*Gr*), aspect ratio of the burner (*l*)), and results have been discussed considering separately laminar, transitional and turbulent flows.

From a methodological point of view, the used experimental set-up has allowed us to overcome the drawbacks of classical systems. The proposed interferometer has demonstrated low sensitivity to geometrical misalignments and high flexibility. This requirements are particularly stringent in consideration of the critical flow features encountered in the experimental investigation of jet flames.

The impact of the line-of-sight integration on the capability to infer flow details have been discussed. In the laminar, steady case (low *Re*), where a cylindrical symmetry of the index of refraction field subsists, local information can be quantitatively restored. In the transitional and turbulent regimes, flow visualizations have pointed out the effect of the decrement of the actual *Re* and the increase of *Ri* associated with heat release, causing large vortical structures to appear. It seems that the energy cascade to finer scales is retarded with respect to isothermal flows, even if the integration along the optical path significantly reduces the capability to deduce insights into the inner spatial structure of the flow.

Based on direct photograph, interferograms and quantitative temperature evaluations in the laminar, steady case, physical aspects of reacting jet flows have been analyzed. The thermal structure of laminar flames has been associated with the phenomenology related to chemical reactions and heat release. Shear layer destabilization develops with a wavy-shaped instability in nonpremixed, transitional jet flames and leads to the formation of large-scale vortical structures. The effect of the buoyancy forces on this process has been also evidenced. In the premixed case, the whole jet dynamics is affected by the structure of the inner reaction zone and the associated heat release, which is in turn determined by the turbulent properties (*Re* and *l*) and by the dilution (ϕ) of the fresh mixture. The outer, large-scale coherent structures evidenced a steady nature in the near field in the considered ranges of the governing parameters, with the exception of the highest *Re* case, where a premixed flame in partial lift-off condition has been visualized.

Acknowledgements

The authors are grateful to Prof. C. Bruno, Mr. E. Giacomazzi and Mr. D. Giordano for their comments on results.

References

Becker, H. A. and Massaro, T. A., Vortex evolution in a round jet, J. Fluid Mech., 31 (1967), 435-448.

Broadwell, J. E. and Mungal, M. G., Large scale structures and molecular mixing, Phys. Fluids, A 3 (5) (1991), 1193-1206.

Carlomagno, G. M., De Luca, L. and Rapillo, A., A new type of interferometer for gas dynamics studies, Proc. 12th Int. Cong. On Instrumentation in Aerospace Simulation Facilities, IEEE Aerospace Electronic Syst. Soc., Williamsburg (1987), 221-226.

Chen, L. D. and Roquemore, W. M., Visualizations of jet flames, Combustion and Flames, 66 (1986), 81-86.

Chomiak, J., Combustion: a study in theory, fact and application, (1990) Abacus Press, New York

Clemens, N. T. and Paul, P. H., Effects of heat release on the near field flow structure of hydrogen jet diffusion flames, Combust. Flames, 102 (1995), 271-284.

Coats, C. M., Coherent structures in combustion, Prog. Energy Combust. Sci., 22 (1996), 427-509.

Eickhoff, H. and Winandy, A., Visualization of vortex formation in jet diffusion flames, Comb Combust. Flames, 60 (1985), 99-101.

Guj, G., Iannetta, S. and Moretti, G., Experimental analysis of thermal fields in horizontally eccentric cylindrical annuli, Ex. Fluids, 12 (1992), 385-393.

Law, C. K., Dynamics of stretched flames, 22th Symposium International On Combustion/The Combustion Institute, (1988), 1381-1402

Merzkirch, W., Flow visualization, (1987), Academic Press. Orlando, Florida.

Mueller, C. J., Driscoll, J. F., Reuss, D. L., Drake, M. C. and Rosalink, M. E., Vorticity generation and attenuation as vortices convect through a premixed flame, Combustion and flame, 112 (1998), 342-358.

Mungal, G. F., Introduction to turbulent combustion, (1999), Lectures series Von Karman Institute, Bruxelles.

Pandya, T. P. and Weinberg, F. J., The structure of flat, counter-flow diffusion flames, Proc. R. Soc. London, (1964), Ser.A 279, 544-561.

Peters, N., The turbulent burning velocity for large-scale and small-scale turbulence, J. Fluid Mech., 384 (1999), 107-132

Poinsot, T., Veynante, D. and Candel, S., Quenching processes and premixed turbulent diagrams, J. Fluid Mech., 228 (1991), 561-606

Stella, A., Guj, G. and Giammartini, S., Measurements of axisymmetric temperature fields using reference beam and shearing interferometry for applications to flames, Accepted for publication in Experiments in Fluids (1999).

Stella, A., Guj, G., Giammartini, S. and Ingenito, G., Assessment for laser velocimetry and thermometry of flames by interferometry, Proc. of the 6th National Symposium of laser velocimetry A.I.VE.LA., Ancona, Italy, (1998).

Vest, C. M., Formation of images from projections: Radon and Abel transforms, J. Opt. Society of America, 64, 9 (1974), 1215-1218.

Weinberg, F. J., Optics of flames, (1963) Butterworth, London.

Yule, A. J., Chigier, N.A., Combustion-transition interaction in a jet flame, AIAA Journal, (1980, June).

Author Profile

Andrea Stella: He received his degree in Aeronautical Engineering from the University of Rome "La Sapienza" in 1997. He is currently carrying out a Ph.D. in Theoretical and Applied Mechanics and the objective of his thesis is the investigation of turbulent combusting flows by means of laser-based diagnostic techniques (PIV, interferometry and LDV). He has been visiting fellow at the DLR (German Aerospace Center) in 1999. Since 1997, his research interests include also hydrodynamic of propellers and rotors and jets in cross streams.

Giulio Guj: He received his degree in Civil Engineering from the University of Rome, in 1975. Research Scientist since 1976 at the Department of Mechanics and Aeronautics of the University of Rome "La Sapienza," Associate Professor of "Experimental and Applied Aerodynamics," University of Rome "La Sapienza," from 1987 to 1992, Associate Professor of "Fluid Dynamics" at University of Rome Three, since 1993.
Scientific Activity: Computational models for Navier Stokes equations by Finite Difference, Finite Element, for application to large Reynolds numbers flows with vector and parallel strategies. Boundary Element methods. Natural or mixed convection flows with complex structure, Rayleigh-Benard problem in 3D limited domains, thermocapillary flows. Two-phase flows, suspensions, flows through cylinder array. Natural convection in anisotropic and isotropic porous medium. Unsteady aerodynamics of rotors and hydrodynamics of propellers. Premixed and non-premixed flames. Statistics and coherent structures in turbulent flows in jets, grids and wakes.

Andrea Mataloni: He received his degree in Aeronautical Engineering from the University of Rome "La Sapienza" in 1999. He is currently working as a consultant engineer at the University "Roma Tre" of Rome on the development and application of optical methods of visualization for the study of combusting and compressible flows.